HOKKAIDO UNIVERSITY

Instructions for use

# Electrochemical Metal Deposition on Top of an Organic Monolayer

## Deyu Qu and Kohei Uosaki*

*Physical Chemistry Laboratory, Division of Chemistry, Graduate School of Science, Hokkaido University, Sapporo 060-0810, Japan*

Electrochemical deposition of metals (platinum or gold) only on top of an organothiolate, 1,4-benzene-dimethanethiol (BDMT) or hexanedithiol (HDT), self-assembled monolayer (SAM) on a Au(111) substrate was achieved by electrochemical reduction of $PtCl_4^{2-}$ or $AuCl_4^-$ ion, which was preadsorbed on one free thiol end group of the dithiol SAM formed on a Au surface, in a metal-ion-free sulfuric acid solution at potentials more negative than the reduction potential of the metal ion. Angle-resolved X-ray photoelectron spectroscopy (AR-XPS) measurement after the reduction of preadsorbed $PtCl_4^{2-}$ ion on BDMT/Au(111) electrode showed the presence of Pt not underneath but on top of the BDMT SAM. After a negative potential scan of the Pt/BDMT/Au(111) electrode to −1.30 V in 0.1 M KOH solution, a typical cyclic voltammogram of a clean Au(111) electrode was obtained, showing that the BDMT SAM with a Pt layer was reductively desorbed. These results proved that a Pt−BDMT SAM−Au substrate sandwich structure without a short circuit between the two metals was successfully constructed by this technique. Furthermore, a decanethiol (DT) monolayer was constructed on a Au layer, which was formed by the reduction of preadsorbed $AuCl_4^-$ ion on HDT/Au(111) electrode. The formation of DT/Au/HDT/Au(111) structure was confirmed as two cathodic peaks corresponding to reductive desorption of DT from Au on top of the HDT/Au(111) at −0.97 V and that of Au/ HDT from Au(111) at −1.12 V were observed when potential was scanned negatively to −1.35 V.

## Introduction

Metal layer formation on top of a nonconductive organic monolayer has been an important research subject in recent years because of its connection with an attractive field of molecular electronics in which an organic monolayer will be used in electronic components. Self-assembled monolayers (SAMs) of thiols are good candidates to be used as molecular layers for this purpose because of their unique advantages such as ease of preparation, highly ordered structure, and well-documented characteristics. To build up molecular devices, attention must be paid to the electrical properties of these organic molecules in the SAM. A metal−SAM−metal sandwich structure without a short circuit between the two metals is used to determine the electrical properties of the molecules and is also an essential component of molecule devices. In this geometry, a Au substrate usually serves as a bottom electrode. The top electrode could be metal nanoclusters prepared by vacuum vapor deposition[1−10] or from a suspension of metal nanoparticles.[11−14] Previous studies have shown that vapor-deposited Au or Ag penetrates into the SAM and inserts into the thiol−Au bond at the Au/SAM interface when it is vacuum-deposited on an alkanethiol SAM with a methyl end group.[2,3,5−7] In contrast, when they are deposited on an alkanedithiol SAM with a thiol end group pointing up, metal nanoparticles are formed on top of the SAM.[1,2,4,8] This is due to the strong interaction between deposited metal nanoparticles and thiol end groups, which reduces the possibility of diffusion of deposited metal nano-particles into the SAM. Dithiol SAMs are also used for attracting and fixing the metal nanoparticles on the surface from a solution.[11−14]

Formation of a metal layer on top of an SAM by electro-chemical deposition has several advantages over vacuum deposition. For example, electrochemical deposition is less complex, less expensive, and easier to control. However, most attempts to electrochemically deposit a metal on top of an SAM have failed. For example, to galvanically deposit copper on thiol-modified Au electrodes, an overpotential is required for nucleation to occur,[15] and defect sites on the SAM act as nucleation centers in the under-potential deposition (UPD) region.[16−18] Deposition of copper took place through these defects, and a Cu monolayer grew between the Au surface and the thiol adlayer.[16−21] The kinetics of this phase formation is very slow, possibly because the deposit has to penetrate through the molecule film and spread out as a buried monolayer.[16−18] In the over-potential deposition (OPD) region, two- and three-dimensional growth of Cu clusters at the defect sites were observed,[16−18,22−24] and the Cu clusters rapidly covered the whole surface.[16−18] In the case of electrochemical deposition of silver on a thiolate SAM-covered Au electrode, Ag ions penetrated the SAM through defects and Ag was deposited directly onto the Au surface.[25,26] While the UPD Ag layer was inserted between the SAM and Au substrate, the thiolate SAM was buried by the bulk Ag deposited at high overpotential.[27] Electrochemical deposition of an Rh cluster on a thiolate-covered Au surface was also studied recently.[28] In that case the imperfections in the SAM acted as nucleation sites for small Rh clusters, and the clusters outgrew on top of the organic monolayer.

The above studies indicate that defect sites in SAMs play a vital role in electrochemical metal deposition on SAM/Au systems, and electrocrystallization of metal initially takes place at these imperfections and metal deposits not on top of but underneath the SAM. This is not surprising since the surface

* To whom correspondence should be addressed. Phone: +81-11-706-3128. Fax: +81-11-706-3440. E-mail: uosaki@pcl.sci.hokudai.ac.jp.
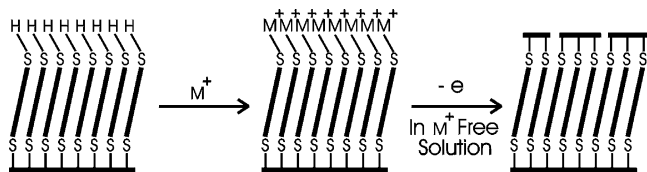
**Figure 1.** Schematic illustration of metal formation on top of the SAM.

energies of metals are higher than those of organic molecules and the metal−metal−SAM configuration is of the lowest energy state.

Another cause of the failure of metal layer formation on top of an SAM by electrochemical metal deposition seems to be the presence of metal ions in solution. Even if some metal ions are immobilized on top of an $\omega$-functional thiolate SAM, such as dithiol, large amounts of free metal ions in the bulk solution can still penetrate the organic film through defect sites in the course of electrochemical reduction reaction, and metal deposition occurs directly on the Au surface.[25,26]

Thus, to deposit metal only on top of an organic surface, at least one of these two factors must be eliminated. Recently, Kolb and co-workers[29−31] demonstrated the formation of a metal layer on an organic surface by electrochemical deposition. They used a 4,4′-dithiodipyridine-modified Au(111) electrode at which a pyridine moiety was exposed, so that palladium(II) or platinum tetrachloride ions were to be adsorbed on the surface of the molecular layer. The Pd or Pt ion was then electrochemically reduced to metallic Pd or Pt in a metal-ion-free acidic solution. They showed that the metal existed not between the SAM and Au substrate but on top of the organic layer by using angle-resolved X-ray photoelectron spectroscopy (XPS). Electrochemical reduction of preadsorbed metal ion in metal-ion-free solution led to the successful deposition of a metal layer only on top of an organic surface.

To wire molecules into an electrical circuit and construct a metal−molecule−metal junction for molecule electronic applications, strong interactions between the molecular layer and the metal layers at each end are required but pyridine−Pt interaction is not necessary strong. Recently, we have proposed another approach,[32] which is closely related to the work of Kolb and co-workers,[29−31] but provides stronger interaction between SAM and the formed metal layer by using dithiol. The adsorption energy of a thiolate group on Pt surface is approximately 65 kcal/mol[33] while that of pyridine with its nitrogen bound to Pt surface is around 18 kcal/mol.[34] There is another advantage of using dithiol SAMs as there are rich references on dithiol SAMs in relation to molecular electronics.[8,11,13,38−42] Thus, the system we studied, metal−dithiol−metal, should be more suitable for application in molecular electronics. The procedure we have proposed for the metal deposition on top of the SAM is schematically described in Figure 1. At first, a Au(111) electrode is modified with a monolayer of dithiol through self-assembly from a solution. The modified electrode is then immersed in a solution containing metal ions. Then the metal ions in the solution bind to the free SH end group of the SAM surface.[35−37] Finally, the electrode is transferred to a metal-ion-free solution, and the adsorbed metal ions are electrochemically reduced to form a metal layer on top of the SAM.

In this work, we carry out the detailed investigation of our approach. Two systems are chosen. One is Pt deposition on a 1,4-benzenedimethanethiol (BDMT) SAM. BDMT is one of the first molecules for which electrical resistance was quantitatively measured,[8,42−44] and the structure, stability, and reactivity of the BDMT SAM on Au have been well studied.[35,45−49] Pt is chosen as the deposited metal by considering the possible application of metal−organic−metal sandwich structure for catalyst.[50] The another system is Au deposition on 1,6-hexanedithiol (HDT). In this case, a second organic layer is formed on the deposited Au to demonstrate the possible construction of organic multilayer.[51]

## Experimental Section

**Materials.** BDMT (>95%) and HDT (>95%) were purchased from TCI (Tokyo Chemical Industry). Methanol (reagent grade), ethanol (reagent grade), $H_2SO_4$ (suprapure grade), $HClO_4$ (suprapure grade), $K_2PtCl_4$ (suprapure grade), and $KAuCl_4$ (96+%) were all obtained from Wako Pure Chemicals. 4-Methylbenzyl mercaptan (MBM, 96%), decanethiol (DT) (>96%), and KOH (semiconductor grade) were purchased from Aldrich. All chemicals were used as received. Water was purified using a Milli-Q purification system (Millipore). Ultrapure Ar gas (99.9995%) was purchased from Air-Water.

A Au(111) single crystal, which was used in electrochemical and XPS measurements, was prepared from a gold wire (99.999% pure, Tanaka Precious Metal) by the Clavilier method[52] and was then cut and mechanically polished. The real surface area of the Au(111) single-crystal electrode was estimated from the cathodic current corresponding to the reduction of Au oxide to be 0.068 cm$^2$. The Au substrates used for ellipsometry measurements were prepared by vacuum evaporation. Titanium of 10 nm in thickness was evaporated on a slide glass at 200 °C followed by 100-nm-thick gold evaporation at an evaporation rate of 0.01 nm s$^{-1}$. The Au surface was flame-annealed in a hydrogen flame and cooled under an argon stream before each measurement.

**Electrochemical Measurements.** Electrochemical measurements were performed in a three-compartment electrochemical cell using a digital potentiostat (Hokuto Denko, HSV-100). The electrode potential was referred to a Ag/AgCl (saturated NaCl) electrode, and a Pt wire was used as a counter electrode. The electrolyte solution was deaerated by bubbling Ar gas for at least 30 min before each experiment.

**Ellipsometry.** Ellipsometry measurements were performed using a SOPRA, GESP-5 ellipsometer in a wavelength region of 300−800 nm with an incident angle upon the sample of 75°. A software program (WINELLI) was employed to determine the monolayer thickness. The refractive index of the SAM was assumed to be 1.45.[53]

**XPS.** XP spectra were obtained using a Rigaku Denki model XPS-7000 X-ray photoelectron spectrometer with a Mg Kα radiation. Base pressure in the analysis chamber was $5 \times 10^{-7}$ Pa. Angle-resolved XP spectra were obtained by varying the angle between the surface and analyzer from 90° to 30°. Wide scans were carried out with 50 eV pass energy, 25 W electron-beam power, and a resolution of 0.8 eV. Narrow-scan spectra of the Pt 4f, S 2p, C 1s, Cl 2p and Au 4f regions were obtained with 15 eV pass energy, 100 W electron-beam power, and a resolution of 0.1 eV. Binding energy was calibrated with an Au 4f$_{7/2}$ peak at 84.0 eV.

**SAM Formation, Metal Ion Adsorption, and Metal Formation.** BDMT, HDT, and MBM SAMs were prepared by immersing the Au substrate in an ethanol solution of thiols with a concentration of 1 mM for 1 or 2 h (for dithiol SAM formation) to 12 h (for monothiol SAM formation). BDMT or HDT-modified gold, after being sufficiently rinsed with ethanol and deionize water, was immersed in 0.5 M KOH solution for 3 min in order to deprotonate the surface thiol group and then

**17572** *J. Phys. Chem. B, Vol. 110, No. 35, 2006*

Qu and Uosaki
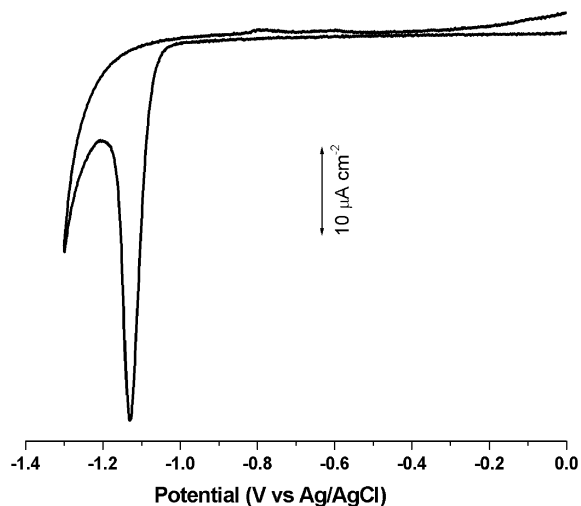


**Figure 2.** Cyclic voltammogram of a BDMT SAM on a Au(111) electrode in a 0.1 M KOH solution with potential scan rate of 20 mV s$^{-1}$.

incubated in 5 mM $K_2PtCl_4$ or $KAuCl_4$ solution for 20 min. The treated Au electrode was transferred to a 0.05 M $H_2SO_4$ solution, and the electrode potential was set at +0.4 V, which is more negative than the redox potential of $PtCl_4^{2-}$ (around +0.55 V) and $AuCl_4^{-1}$ (around +0.8 V),[54] to electrochemically reduce the adsorbed Pt or Au ions to metallic Pt or Au, respectively, on top of the BDMT or HDT SAM.

## Results and Discussion

**Characterization of BDMT SAM.** Previous studies showed that BDMT is adsorbed on a Au surface with a benzene ring perpendicular to the surface.[35,45−49] In this orientation, one thiol group binds to the Au surface and the other is free on the surface. This free thiol group on the surface may lead to the formation of a multilayer as indicated by previous studies.[35,45−49] The formed BDMT SAM on the Au(111) surface was characterized by ellipsometry and cyclic voltammetry.

The measured ellipsometric thicknesses of BDMT layers on a vacuum-evaporated Au substrate surface with self-assembly in a 1 mM BDMT ethanol solution for 1, 2, and 3 h were found to be 1.1 ± 0.2 nm, 1.0 ± 0.20 nm, and 1.5 ± 0.2 nm, respectively. The expected thickness of a BDMT monolayer film on Au with perpendicular orientation, taking into account the molecular length, bond angle, and Au−S bond distance, is 1.14 nm.[45,49] Thus, a BDMT SAM formed on an Au(111) surface prepared under the present conditions was a monolayer with perpendicular orientation, leaving one free SH group on top of the SAM.

A cyclic voltammogram (CV) of a BDMT SAM on Au(111) was recorded in a 0.1 M KOH solution with a potential scan rate of 20 mV s$^{-1}$ as shown in Figure 2. A sharp cathodic peak corresponding to reductive desorption of the BDMT SAM was observed at −1.13 V. The reductive charge was 100 $\mu C$ cm$^{-2}$ without double-layer charge correction, which is in good agreement with the value for the reductive desorption of an alkanethiolate SAM with saturated coverage of a ($\sqrt{3} \times \sqrt{3}$) $R$ 30° structure formed on an Au(111) surface.[55−59] It should be mentioned that this value consists of 70% of Faradic charge for one-electron reduction of an SAM with saturated coverage of a ($\sqrt{3} \times \sqrt{3}$) $R$ 30° structure and 30% of capacitive (non-Faradic) charge.[55−59]

These observations suggest that a full monolayer of BDMT was formed on the Au(111) surface with a free thiol end group face up.[35,45−49]
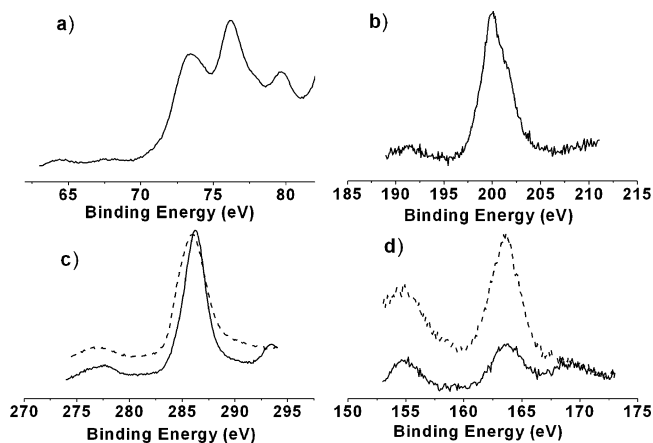


**Figure 3.** XP spectra of (a) Pt 4f, (b) Cl 2p, (c) C 1s, and (d) S 2p regions of a BDMT SAM before (dashed line) and after (solid line) Pt complex ion adsorption.

**Adsorption of Platinum Ions on BDMT SAM Surface.** Figure 3 shows XP spectra of a Pt-ion-modified BDMT SAM on a Au(111) substrate. The XPS spectra in Pt 4f region (Figure 3a) clearly show a Pt 4f doublet with binding energy of Pt 4f$_{7/2}$ and Pt 4f$_{5/2}$ peaks at 72.9 and 75.6 eV, respectively. The Cl 2p (Figure 3b) peak was observed at a binding energy of 200.1 eV, which agrees with that of Cl 2p of $K_2PtCl_4$.[60] The relative amount of Pt and Cl was determined by[61]

$$C_{Cl}/C_{Pt} = (I_{Cl}/R_{Cl})/(I_{Pt}/R_{Pt}) \tag{1}$$

where $I$ is the peak intensity and $R$ is the relative sensitivity factor. Using $R_{Cl}$ and $R_{Pt}$ of 0.45 and 1.75, respectively,[61] the ratio of Cl to Pt ($C_{Cl}/C_{Pt}$) was found to be 3.8. These results and the fact that no potassium peak was found in the XP spectra indicate that the platinum ions were adsorbed on the SAM in the form of platinum tetrachloride complex ($PtCl_4^{2-}$). The obtained binding energy of Pt 4f$_{7/2}$ was smaller than 73.4 eV, which corresponds to Pt 4f$_{7/2}$ binding energy of $K_2PtCl_4$.[61] This suggests that Pt was coordinated with the S end group and that the oxidation state of Pt was changed from +2 to +1.[35,37] As shown in Figure 3c, the XP spectra in the C 1s region before (dashed line) and after (solid line) adsorption of Pt ions are almost identical with a binding energy peak of 285.7 eV. This implies that the attachment of Pt ions did not affect the amount and the nature of BDMT SAM.

Figure 3d shows XP spectra in the S 2p region before (dashed line) and after (solid line) adsorption of Pt ions. The position of the S 2p peak before the adsorption Pt ions was 164 eV, which is in good agreement with that of a dithiol SAM-covered Au,[62,63] where two types of sulfur species, i.e., Au−SR and RSH, coexisted. After adsorption of Pt ions, the S 2p peak was observed at slightly lower binding energy with a shoulder around 162.5 eV and seemed to be broadened with decreased intensity. This suggests that thiol, with S 2p$_{3/2}$ and S 2p$_{1/2}$ peaks at 163.6 and 164.8 eV, respectively,[63,64] was converted to thiolate, with S 2p$_{3/2}$ and S 2p$_{1/2}$ peaks at 161.9 and 163.1 eV, respectively,[63,64] after the Pt ion adsorption. This clearly indicates that the free thiol groups on the surface have been coordinated with platinum complex ions.

**Formation of Metallic Pt on Top of the BDMT SAM Surface.** Figure 4 shows a cyclic voltammogram of the Pt-ion-modified BDMT SAM-covered Au(111) electrode recorded in 0.05 M $H_2SO_4$ solution after electrochemical reduction of platinum ions in 0.05 M $H_2SO_4$ solution by holding the electrode

Electrochemical Metal Deposition on Top of SAM

*J. Phys. Chem. B, Vol. 110, No. 35, 2006* **17573**
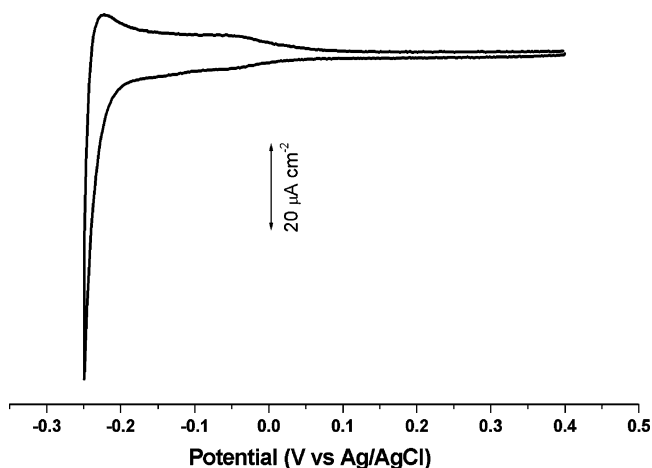


**Figure 4.** Cyclic voltammogram of a Pt/BDMT/Au electrode in 0.05 M $H_2SO_4$ solution with potential scan rate of 20 mV s$^{-1}$

.



**Figure 5.** XP spectra of electrodes prepared in different steps (BDMT/ Au: dashed line; Pt ion/BDMT/Au: dotted line; Pt/BDMT/Au: solid line) in the region of (a) Pt 4f, (b) Cl 2p, (c) C 1s, and (d) S 2p.

potential at $+0.4$ V. A redox wave was observed in the potential region of $+0.1$ V to $-0.20$ V, and a significant increase of cathodic current was observed at potentials more negative than $-0.2$ V. This is a typical CV of a Pt electrode, and no peaks were found in this potential region at the BDMT SAM-covered Au(111) electrode in the same solution, confirming the redox wave observed in Figure 4 is not due to reductive desorption/ oxidative readsorption of the BDMT SAM but adsorption/ desorption of hydrogen on Pt. The large cathodic current was due to hydrogen evolution. These results prove that metallic Pt was formed.

The charge associated with the desorption of hydrogen on the electrochemically deposited Pt was found to be 61 $\mu$C cm$^{-2}$. This value is equal to about 28% of the charge associated with the desorption of one hydrogen full monolayer on a Pt(111) surface, which is 210 $\mu$C cm$^{-2}$,[65] suggesting that only $^1/_3$ monolayer of Pt with respect to the number of gold atoms on the Au(111) surface was formed. This is in very good agreement with the value expected from the structure of thiolate SAM on Au(111), i.e., $(\sqrt{3} \times \sqrt{3})$ R 30° structure, in which the number of molecules with respect to the number of gold atoms on the Au(111) surface is 1/3. These results suggest that one free thiol group of each dithiol molecule is linked to one platinum tetrachloride complex ion.

Figure 5 shows XP spectra of a Pt−BDMT−Au(111) electrode. Peaks of Pt 4f$_{7/2}$ and Pt 4f$_{5/2}$ were observed at 71.7 and 75.2 eV, respectively (solid line), which are shifted from 72.9 and 75.6 eV, respectively (dotted line), obtained before the reduction, confirming that metallic Pt was formed. The binding energies of Pt 4f$_{7/2}$ and Pt 4f$_{5/2}$ peaks in Figure 5a are still higher than those of the bulk Pt metal, i.e., 71.2 and 74.5 eV, respectively.[61] A similar shift was reported in the XP spectra of alkylthiol-modified Pt nanoclusters, in which the Pt 4f binding energies were found to be higher than those of bulk Pt by 0.8 eV.[66] Figure 5b shows that the Cl 2p peak totally disappeared after electrochemical reduction of Pt ions. This also supports that the Pt complex ions were reduced to metallic Pt. The C 1s spectra before and after the reduction were, however, almost identical as shown in Figure 5c, showing that the BDMT SAM was not disturbed in the course of Pt metal formation. The position of the S 2p peak (Figure 5d) was also found to be the same before and after the electrochemical reduction.

Figure 6 shows a set of XP spectra of a Pt−BDMT−Au-(111) electrode in the region of (a) Pt 4f and Au 4f$_{7/2}$, (b) C 1s,
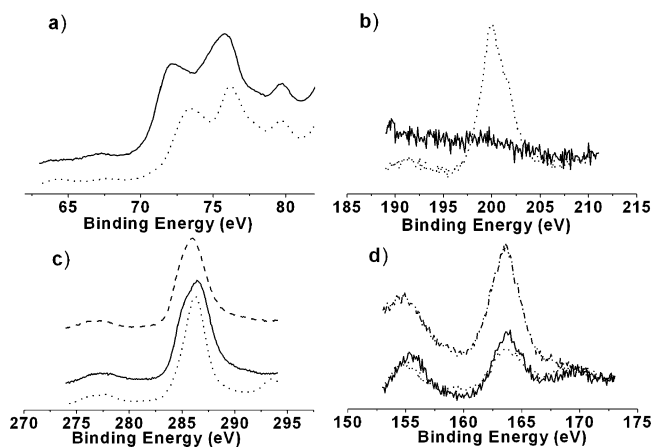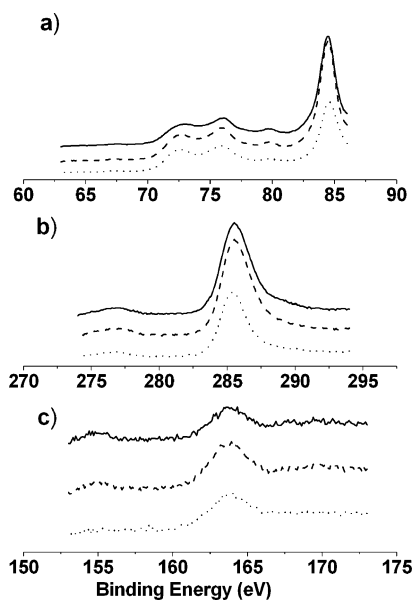


**Figure 6.** XP spectra of Pt/BDMT/Au electrodes with different exit angles (90°: solid line, 60°: dashed line, 30°: dotted line) in the region of (a) Pt 4f with Au 4f$_{7/2}$ peak, (b) C 1s, and (c) S 2p.

and (c) S 2p observed with various takeoff angles, $\theta$, i.e., angles between the electrode surface and the direction of photoelectrons detected by the analyzer. The intensities of the Au 4f$_{7/2}$ peak with binding energy of 84 eV and C 1s peak with binding energy of 285.7 eV decreased with decrease in the takeoff angle. On the other hand, the intensity of Pt 4f with binding energy of 72.9 and 75.6 eV seems to be independent of the takeoff angle. The intensities of the S 2p peak were also found to be constant at different takeoff angles. To clearly see the relation between the relative intensities of the Pt 4f peak with respect to the Au 4f$_{7/2}$ and C 1s peaks and the takeoff angles, log($I_{Pt}/I_{Au}$) and log-($I_{Pt}/I_C$) were plotted as a function of $1/\sin \theta$ in Figure 7. The relative intensities of the Pt 4f peak to those of the Au 4f and C 1s peaks increased as the takeoff angle decreased. This proves that Pt was indeed deposited not underneath but *on top of* the BDMT SAM.

The results of electrochemical measurements also provided the evidence that Pt was present *only on top of* the SAM. A solid line in Figure 8 shows a current response of the Pt−BDMT SAM-modified Au(111) electrode at the first cycle of the
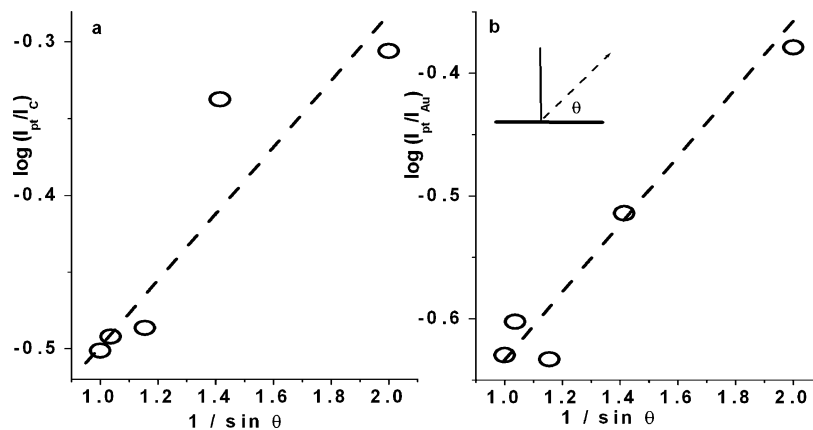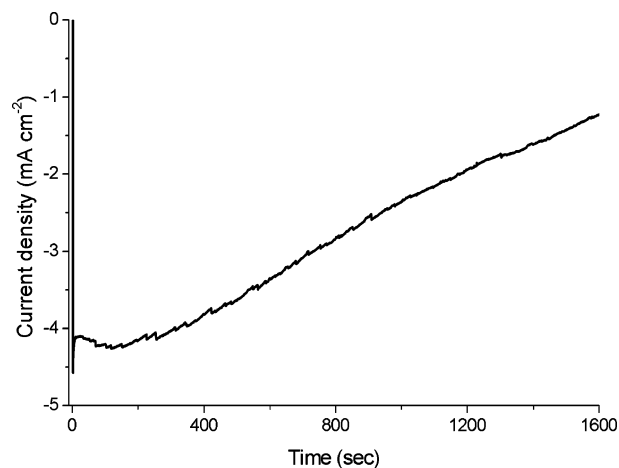
**Figure 7.** Dependencies of relative intensity of (a) $I_{Pt}/I_{Au}$ and (b) $I_{Pt}/I_C$ on the takeoff angle. $I_{Pt}$, $I_{Au}$, and $I_C$ represent the intensities of XP spectra of Pt $4f_{7/2}$, Au $4f_{7/2}$, and C 1s peaks, respectively.
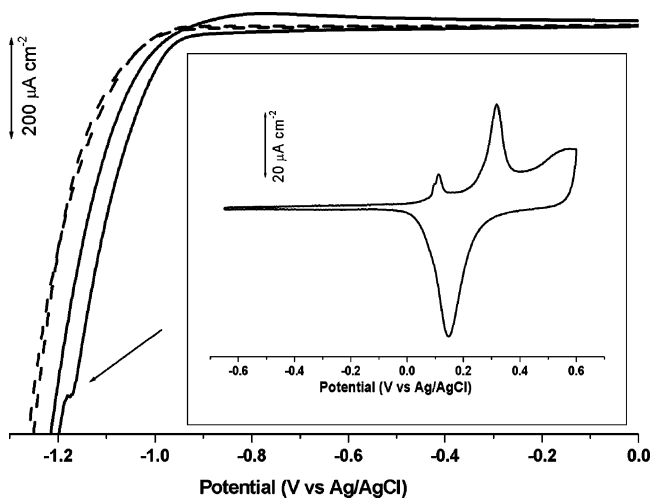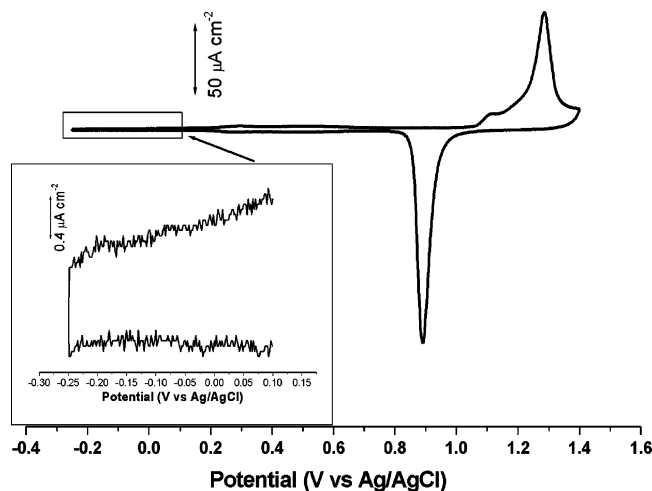


**Figure 8.** Cyclic voltammogram of a Pt/BDMT/Au electrode recorded in 0.1 M KOH solution with potential scan rate of 20 mV s$^{-1}$. Solid line shows the first cycle of potential scan between 0 and −1.30 V. Dashed line shows the second cycle of scan. Inset: A CV of the electrode, after above-mentioned scans, in the potential region between −0.6 V and +0.6 V.



**Figure 9.** Current response of the Pt/BDMT/Au(111) electrode vs time after potential stepped from 0 V to −1.30 V in 0.1 M KOH solution.

potential scan in the region between 0 and −1.30 V. The cathodic current increased significantly when the potential became more negative than −1.0 V, and a shoulder peak was observed at −1.18 V. The large cathodic current is due to hydrogen evolution. It is well-known that Pt has much higher catalytic activities for hydrogen evolution reaction (HER) than Au.[67] The hydrogen evolution current at Au(111) electrode in 0.1 M KOH solution started to flow around −1.1 V. The shoulder should be due to the desorption of the Pt covered BDMT SAM. The position of the shoulder peak is more negative than the reductive desorption peak potential of the BDMT SAM. The reductive charge of this peak is not able to be estimated accurately because it is not possible to separate it from the charge of hydrogen evolution. The HER current at a given potential was smaller in the reverse scan. The dashed line in Figure 8 shows the current response of the electrode during the second cycle of the potential scan in the same potential region. It clearly shows that the HER current decreased further in this scan, showing that the amount of Pt gradually decreased. These results indicate that Pt−BDMT SAM was desorbed from the electrode surface in the negative going scan of the first potential cycle but stayed in the vicinity of the electrode and gradually left from the surface. To confirm the removal Pt from the

electrode, current response of the Pt−BDMT SAM-modified Au(111) electrode was recorded when the potential was stepped from 0 V to −1.30 V in 0.1 M KOH solution (Figure 9). The current decreased gradually with time, confirming that Pt was remained in the vicinity of the electrode after desorption of Pt−BDMT SAM and gradually diffused away. It is already known that thiol molecules form aggregate on the surface after the reductive desorption.[55−57,68−70] The inset of Figure 8 shows a CV of the Pt−BDMT SAM-modified electrode after above-mentioned potential scans in the potential region between −0.6 V and +0.6 V. This is a typical CV of a clean Au(111) electrode in a 0.1 M KOH solution,[55,71] suggesting the total removal of the Pt−BDMT layer and recovery of the clean Au(111) surface by potential cycling. The recovery of the clean Au(111) surface was further confirmed by the CV of the electrode recorded in H$_2$SO$_4$ solution after the examination in 0.1 M KOH solution as shown in Figure 10, which is also in good agreement with that of a clean Au(111) electrode reported previously.[72,73] The inset of Figure 10 shows the current−voltage relation with enlarged scale in the potential region between +0.1 V and −0.25 V. It is clear that no redox wave of hydrogen adsorption/ desorption at Pt electrode was observed, no sign of HER in this potential region. It should be stressed that even small amount of Pt on a Au electrode significantly enhances the HER current, which can be easily detected. Furthermore, the XP spectra obtained after the negative scan to −1.30 V in 0.1 M KOH solution show no Pt 4f and S 2p peaks. These results clearly

**Figure 10.** Cyclic voltammogram of the electrode after desorbing the Pt/BDMT SAM recorded in 0.05 M H$_2$SO$_4$ solution with a potential scan rate of 20 mV s$^{-1}$. Inset: An enlarged scale in the potential region between +0.1 and −0.25 V.



**Figure 11.** CV of a Pt-deposited BDMT SAM-modified Au(111) electrode, which was prepared in a 0.05 M H$_2$SO$_4$ solution containing PtCl$_4^{2-}$ ions at +0.4 V, measured in 0.05 M H$_2$SO$_4$ solution with a scan rate of 20 mV s$^{-1}$ after the reductive desorption of the BDMT SAM in a 0.1 M KOH solution by scanning the potential to −1.30 V.

show that Pt was removed with BDMT by the cathodic scan in alkaline solution, indicating that Pt was not deposited on the Au(111) surface but existed *only on top of* the SAM and that the Pt−SAM was reductively desorbed as it is impossible to remove it by negative potential scan if Pt was directly deposited on Au.

**Electrochemical Pt Deposition on a BDMT SAM in a Solution Containing Platinum Ions and on an MBM SAM in a Platinum-Ion-Free Solution.** The above results show that a Pt/SAM/Au sandwich structure without a short circuit between two metals can be constructed by the method proposed here. There seems to be two important key factors for the success. One of the key factors in this method is that the reductive deposition of metal was carried out in a metal-ion-free solution. This prevents the diffusion of free metal ions through the organic film to the Au substrate surface. Another key factor is the presence of free thiol end groups on the SAM, which provide adsorption sites for metal ions. This prevents the penetration of metal ions through the SAM and metal being deposited underneath of the SAM, directly on the substrate metal.

To confirm the importance of these factors, effects of excess platinum ion and of free thiol end group were investigated by studying electrochemical deposition of Pt on a BDMT SAM-modified Au(111) surface in a solution containing platinum ions and on an MBM SAM-modified Au(111) surface in a platinum-ion-free solution, respectively.

Pt deposition on a BDMT-covered Au(111) electrode was carried out in a 0.05 M H$_2$SO$_4$ solution containing PtCl$_4^{2-}$ ions at +0.4 V. After holding the potential at 0.4 V for 20 min, which is equal to the incubation time used for Pt deposition in a Pt-ion-free solution, the electrode was transferred to 0.1 M KOH solution and potential was scanned negatively to −1.3 V so that BDMT SAM was reductively desorbed. Figure 11 shows a CV of this electrode after the reductive desorption of the SAM in 0.1 M KOH solution measured in a 0.05 M H$_2$SO$_4$ solution. In contrast to the result obtained for the Pt−BDMT−Au(111) electrode prepared in a Pt-ion-free solution shown in Figure 10, a cathodic peak corresponding to the reduction of platinum oxide and a hydrogen adsorption/desorption wave were observed at around 0.4 V and in the potential region of +0.1V to −0.20 V, respectively. This clearly shows that Pt remained on the Au surface after reductive desorption of the BDMT SAM, indicating
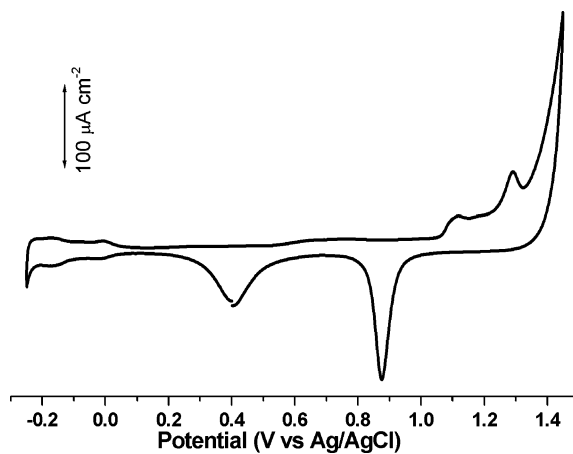
that Pt was deposited directly on the Au surface if Pt deposition on a BDMT-covered Au(111) electrode was carried out in a solution containing platinum ion. Thus, it is proved that the platinum-ion-free solution is one of the key factors for the formation of a metal−molecule−metal structure without short circuit as suggested above.

Pt deposition was also carried out on an MBM SAM-modified Au(111) electrode in a similar way as for Pt deposition on a BDMT SAM-modified Au(111) electrode. After the incubation in 5 mM K$_2$PtCl$_4$ solution for 20 min, the MBM SAM-modified Au(111) electrode was transferred to a 0.05 M H$_2$SO$_4$ solution, i.e., platinum-ion-free solution, and then the electrode potential was set at +0.4 V so that adsorbed PtCl$_4^{2-}$ was electrochemically reduced to metallic Pt. After these treatments, the electrode was transferred to a 0.1 M KOH solution where reductive desorption of the SAM was carried out by scanning the potential to −1.30 V. A CV of this electrode after the reductive desorption measured in a 0.05 M H$_2$SO$_4$ solution was similar to the one shown in Figure 11, indicating that Pt still existed on the Au surface. This indicates that the Pt ions diffused through the SAM in the course of incubation and adsorbed on the Au(111) surface. The adsorbed PtCl$_4^{2-}$ was electrochemically reduced to metallic Pt on the Au surface. Thus, importance of the existence of free thiol end groups to prevent the direct deposition of Pt on the Au substrate was also proved.

**Electrochemical Formation of Metallic Au on Top of HDT SAM-Covered Au(111) Surface.** To prove this method is applicable for the deposition of not only Pt but also other metals on organic monolayers, Au was also electrochemically deposited on top of an HDT SAM surface. Since the deposited metal is the same material as the bottom substrate, the XPS measurements were not carried out. Electrochemical and ellipsometry measurements showed that a full monolayer of HDT with measured ellipsometric thicknesses about 0.84 nm, which is close to the expected length of 0.80 nm for the all-trans HDT monolayer with a 30° tilt angle,[74] was formed on a Au(111) surface. After reduction of the adsorbed AuCl$_4^{-1}$, metallic Au was considered to be deposited on top of an HDT SAM-covered Au(111) surface. To prove this, the Au/HDT/Au(111) structure was used for an organic bilayer formation.[51] Figure 12 shows a CV of the Au/HDT/Au(111) electrode after the electrode was dipped in an ethanol solution containing 1 mM DT recorded in a 0.1 M KOH solution in a potential region between 0 and −1.35
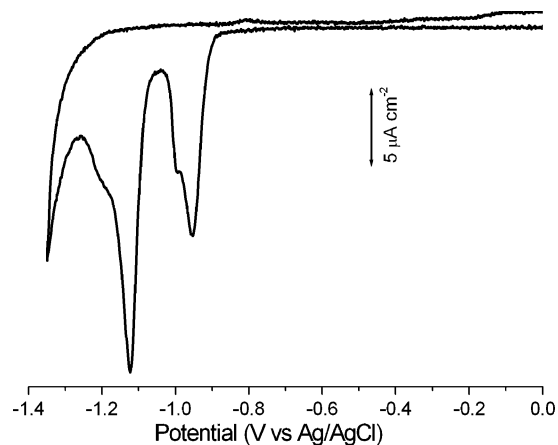
**Figure 12.** Cyclic voltammogram of a DT/Au/HDT on Au(111) electrode in 0.1 M KOH solution with a scan rate of 20 mV s$^{-1}$.

V. In contrast to the results shown in Figure 8, clearly resolved two cathodic peaks were observed at $-0.97$ and $-1.12$ V because HER was not catalyzed by deposited Au and took place at more negative potential than the desorption of the SAMs. The peak position of the reductive desorption of HDT SAM after the Au deposition was close to that of the latter peak and was more negative than that of reductive desorption of HDT SAM, suggesting that the latter peak was due to the reductive desorption of the Au/HDT SAM from the Au(111) substrate. The charges of the former and the latter reduction peaks were 35 and 101 $\mu$C cm$^{-2}$, respectively, without double-layer charge correction. Since the total reductive charge of the two peaks was much larger than that of the reductive desorption of a full-monolayer of alkanethiolate SAM on a Au(111) surface, the possibility that the appearance of these two peaks was due to the formation of binary SAM on the Au(111) surface by the replacement of Au/HDT SAM with DT in solution was ruled out.[75,76] These results suggest that the former peak at $-0.97$ V was due to the reductive desorption of DT SAM from the deposited Au on HDT modified Au(111) electrode. The fact that the charge of the former peak was 34% of the latter is reasonably explained by considering that the amount of Au atoms deposited on HDT modified Au(111) surface was similar to that of Pt atoms deposited on the BDMT SAM, which was ca. $\frac{1}{3}$ of the Au atoms on the (111) surface. The DT SAM was desorbed at more positive potential than the Au/HDT SAM because while DT SAM was exposed to the solution, HDT SAM was buried.

**Conclusions**

We have constructed and characterized metal$-$SAM$-$Au sandwich structures. A dithiol SAM with free thiol groups facing up was first formed on a Au(111) surface, metal ions were then adsorbed on the free thiol groups of the thiol-terminated SAM surface, and finally the metal ions were electrochemically reduced in a metal-ion-free solution to form metal layer on top of the dithiol SAM surface. XPS and electrochemical measurements confirmed that metal was deposited not directly on the Au(111) surface but only on top of the SAM. The strong interaction between metal ions and the thiol-terminated surface as well as the use of a metal-ion-free solution prevented the deposition of metal on the Au(111) surface, i.e., beneath the SAM. Bilayer structure was also constructed by utilizing Au/SAM/Au(111) structure. Investigations of the electronic and catalytic properties of metals deposited on the SAM are underway.

**References and Notes**

(1) Boer, B.; Frank, M. M.; Chabal, Y. J.; Jiang, W.; Garfunkel, E.; Bao, Z. *Langmuir* **2004**, *20*, 1539.
(2) Ohgi, T.; Sheng, H.-Y.; Nejoh, H. *Appl. Surf. Sci.* **1998**, *130−132*, 919.
(3) Ohgi, T.; Sheng, H.-Y.; Dong, Z.-C.; Nejoh, H. *Surf. Sci.* **1999**, *442*, 277.
(4) Ohgi, T.; Sheng, H.-Y.; Dong, Z.-C.; Nejoh, H.; Fujita, D. *Appl. Phys. Lett.* **2001**, *79*, 2453.
(5) Esplandiu, M. J.; Noeske, P.-L. M. *Appl. Surf. Sci.* **2002**, *199*, 166.
(6) Tarlov, M. J. *Langmuir* **1992**, *8*, 80.
(7) Ohgi, T.; Fujita, D.; Deng, W.; Dong, Z.-C.; Nejoh, H. *Surf. Sci.* **2001**, *493*, 453.
(8) Andres, R. P.; Bein, T.; Dorogi, M.; Feng, S.; Henderson, J. I.; Kubiak, C. P.; Mahoney, W.; Osifchin, R. G.; Reifenberger, R. *Science* **1996**, *272*, 1323.
(9) Speets, E. A.; Ravoo, B. J.; Roesthuis, F. J. G.; Vroegindeweij, F.; Blank, D. H. A.; Reinhoudt, D. N. *Nano Lett.* **2004**, *4*, 841.
(10) Speets, E. A.; Dordi, B.; Ravoo, B. J.; Oncel, N.; Hallback, A.-S.; Zandvliet, H. J. W.; Poelsema, B.; Rijnders, G.; Blank, D. H. A.; Reinhoudt, D. N. *Small* **2005**, *1*, 395.
(11) Cui, X. D.; Primak, A.; Zarate, X.; Tomfohr, J.; Sankey, O. F.; Moore, A. L.; Moore, T. A.; Gust, D.; Harris, G.; Lindsay, S. M. *Science* **2001**, *294*, 571.
(12) Xiao, Y.; Patolsky, F.; Katz, E.; Hainfeld, J. F.; Willner, I. *Science* **2003**, *299*, 1877.
(13) Ramachandran, G. K.; Hopson, T. J.; Rawlett, A. M.; Nagahara, L. A.; Primak, A.; Lindsay, S. M. *Science* **2003**, *300*, 1413.
(14) Zheng, J.; Zhou, Y.; Li, X.; Ji, Y.; Lu, T.; Gu, R. *Langmuir* **2003**, *19*, 632.
(15) Sondag-Huethorst, J. A. M.; Fokkink, L. G. J. *Langmuir* **1995**, *11*, 4823.
(16) Hagenström, H.; Schneeweiss, M. A.; Kolb, D. M. *Langmuir* **1999**, *15*, 7802.
(17) Hagenström, H.; Schneeweiss, M. A.; Kolb, D. M. *Electrochim. Acta* **1999**, *45*, 1141.
(18) Baunach, T.; Kolb, D. M. *Anal. Bioanal. Chem.* **2002**, *373*, 743.
(19) Nishizawa, M.; Sunagawa, T.; Yoneyama, H. *Langmuir* **1997**, *13*, 5215.
(20) Oyamatsu, D.; Nishizawa, M.; Kuwabata, S.; Yoneyama, H. *Langmuir* **1998**, *14*, 3298.
(21) Epple, M.; Bittner, A. M.; Kuhnke, K.; Kern, K.; Zheng, W.-Q.; Tadjeddine, A. *Langmuir* **2002**, *18*, 773.
(22) Gilbert, S. E.; Cavalleri, O.; Kern, K. *J. Phys. Chem.* **1996**, *100*, 12123.
(23) Cavalleri, O.; Gilbert, S. E.; Kern, K. *Surf. Sci.* **1997**, *377−379*, 931.
(24) Cavalleri, O.; Gilbert, S. E.; Kern, K. *Chem. Phys. Lett.* **1997**, *269*, 479.
(25) Esplandiu, M. J.; Hagenstrom, H. *Solid State Ionics* **2002**, *150*, 39.
(26) Esplandiu, M. J. *Probe Microsc.* **2001**, *2*, 89.
(27) Hagenström, H.; Esplandiu, M. J.; Kolb, D. M. *Langmuir* **2001**, *17*, 839.
(28) Langerock, S.; Ménard, H.; Rowntree, P.; Heerman, L. *Langmuir* **2005**, *21*, 5124.
(29) Baunach, T.; Ivanova, V.; Kolb, D. M.; Boyen, H.-G.; Ziemann, P.; Buttner, M.; Oelhafen, P. *Adv. Mater.* **2004**, *16*, 2024.
(30) Ivanova, V.; Baunach, T.; Kolb, D. M. *Electrochim. Acta* **2005**, *50*, 4283.
(31) Manolova, M.; Ivanova, V.; Kolb, D. M.; Boyen, H.-G.; Ziemann, P.; Buttner, M.; Romanyuk, A.; Oelhafen, P. *Surf. Sci.* **2005**, *590*, 146.
(32) Qu, D.; Uosaki, K. *Chem. Lett.* **2006**, *35* (3), 258.
(33) Geng, W. T.; Nara, J.; Ohno, T. *Thin Solid Films* **2004**, *464−465*, 379.
(34) de Souza, P. R. N.; Aranda, D. A. G.; Carneiro, J. W. de M.; de Oliveira, C. da S. B.; Antunes, O. A. C.; Passos, F. B. *Int. J. Quat. Chem.* **2003**, *92*, 400.
(35) Burst, M.; Blass, P. M.; Bard, A. J. *Langmuir* **1997**, *13*, 5602.
(36) Deng, W.; Yang, L.; Fujita, D.; Nejoh, H.; Bai, C. *Appl. Phys. A* **2000**, *71*, 639.

Electrochemical Metal Deposition on Top of SAM

*J. Phys. Chem. B, Vol. 110, No. 35, 2006* **17577**

(37) Venkataramanan, M.; Murty, K. V. G. K.; Pradeep, T.; Deepali, W.; Vijayamohanan, K. *Langmuir* **2000**, *16*, 7673.

(38) Wynn, C. M.; Fedynshyn, T. H.; Geis, M. W.; Kunz, R. R.; Lyszczarz, T. M.; Rothschild, M.; Spector, S. J.; Switkes, M. *Nanotechnology* **2004**, *15*, 86.

(39) Piccinin, S.; Selloni, A.; Scandolo, S.; Car, R.; Scoles, G. *J. Chem. Phys.* **2003**, *119*, 6729.

(40) Engelkes, V. B.; Beebe, J. M.; Frisbie, C. D. *J. Am. Chem. Soc.* **2004**, *126*, 14287.

(41) Cai, L. T.; Skulason, H.; Kushmerick, J. G.; Pollack, S. K.; Naciri, J.; Shashidhar, R.; Allara, D. L.; Mallouk, T. E.; Mayer, T. S. *J. Phys. Chem. B* **2004**, *108*, 2827.

(42) Dadosh, T.; Gordin, Y.; Krahne, R.; Khivrich, L.; Mahalu, D.; Frydman, V.; Sperling, J.; Yacoby, A.; Bar-Joseph, I. *Nature* **2005**, *436*, 677.

(43) Dorogi, M.; Gomez, J.; Osifchin, R.; Andres, R. P.; Reifenberger, R. *Phys. Rev. B* **1995**, *52*, 9071−9077.

(44) Xiao, X.; Xu, B.; Tao, N. J. *Nano Lett.* **2004**, *4*, 267.

(45) Joo, S. W.; Han, S. W.; Kim, K. *J. Phys. Chem. B* **1999**, *103*, 10831.

(46) Murty, K. V. G. K.; Venkataramanan, M.; Pradeep, T. *Langmuir* **1998**, *14*, 5446.

(47) Pugmire, D. L.; Tarlov, M. J.; Zee, R. D. V.; Naciri, J. *Langmuir* **2003**, *19*, 3720.

(48) Sur, U. K.; Subramanian, R.; Lakshminarayanan, V. *J. Colloid Interface Sci.* **2003**, *266*, 175.

(49) Vandamme, N.; Snauwaert, J.; Janssens, E.; Vandeweert, E.; Lievens, P.; Haesendonck, C. V. *Surf. Sci.* **2004**, *558*, 57.

(50) St.-Pierre, G.; Chagnes, A.; Bouchard, N. A.; Harvey, P. D.; Brossard, L.; Ménard, H. *Langmuir* **2004**, *20*, 6365.

(51) Qu, D.; Ito, M.; Noguchi, H.; Uosaki, K. In preparation.

(52) Clavilier, J.; Faure, R.; Guinet, G.; Durand, R. *J. Electroanal. Chem.* **1980**, *107*, 205.

(53) Ulman, A. *An introduction to ultra-thin organic films from Langmuir−Blodgett to self-assembly*; Academic Press: San Diego, CA, 1991.

(54) Bard, A. J.; Faulkner, L. R. *Electrochemical Methods*—Fundamentals and Applications, 2nd ed.; John Wiley & Sons: New York, 2000.

(55) Yang, D.-F.; Wilde, C. P.; Morin, M. *Langmuir* **1996**, *12*, 6570.

(56) Yang, D.-F.; Wilde, C. P.; Morin, M. *Langmuir* **1997**, *13*, 243.

(57) Qu, D.; Morin, M. *J. Electroanal. Chem.* **2001**, *517*, 45.

(58) Sumi, T.; Wano, H.; Uosaki, K. *J. Electroanal. Chem.* **2003**, *550-551*, 321.

(59) Sumi, T.; Uosaki, K. *J. Phys. Chem. B* **2004**, *108*, 6422.

(60) Bremi, J.; Brovelli, D.; Caseri, W.; Hahner, G.; Smith, P.; Tervoort, T. *Chem. Mater.* **1999**, *11*, 977.

(61) *Handbook of X-ray Photoelectron Spectroscopy*; JEOL, 1991.

(62) Nakanishi, T.; Ohtani, B.; Shimazu, K.; Uosaki, K. *Chem. Phys. Lett.* **1997**, *278*, 233.

(63) Nakanishi, T.; Ohtani, B.; Uosaki, K. *J. Phys. Chem. B* **1998**, *102*, 1571.

(64) Laibinis, P. E.; Whitesides, G. M.; Allara, D. L.; Tao, Y.-T.; Parikh, A. N.; Nuzzo, R. G. *J. Am. Chem. Soc.* **1991**, *113*, 7152.

(65) Trassati, S.; Petrii, O. A. *Pure Appl. Chem.* **1991**, *63*, 712.

(66) Fu, X.; Wang, Y.; Wu, N.; Gui, L.; Tang, Y. *J. Colloid Interface Sci.* **2001**, *243*, 326.

(67) Bockris, J. O'M.; Reddy, A. K. N.; Gamboa-Aldeco, M. *Modern Electrochemistry*, 2nd ed.; Kluwer Academic/Plenum Publishers: New York, 2000.

(68) Yang, D.-F.; Al-Maznai, H.; Morin, M. *J. Phys. Chem. B* **1997**, *101*, 1158.

(69) Byloos, M.; Al-Maznai, H.; Morin, M. *J. Phys. Chem. B* **1999**, *103*, 6554.

(70) Hobara, D.; Miyake, K.; Imabayashi, S.; Niki, K.; Kakiuchi, T. *Langmuir* **1998**, *14*, 3590.

(71) Hamelin, A.; Sottomayor, M. J.; Silva, F.; Chang, S.-C.; Weaver, M. J. *J. Electroanal. Chem.* **1990**, *295*, 291.

(72) Angerstein-Kozlowska, H.; Conway, B. E.; Hamelin, A.; Stoicoviciu, L. *J. Electroanal. Chem.* **1987**, *228*, 429.

(73) Hamelin, A. *J. Electroanal. Chem.* **1996**, *407*, 1.

(74) Kohli, P.; Taylor, K. K.; Harris, J. J.; Blanchard, G. J. *J. Am. Chem. Soc.* **1998**, *120*, 11962.

(75) Kakiuchi, T.; Sato, K.; Iida, M.; Hobara, D.; Imabayashi, S.; Niki, K. *Langmuir* **2000**, *16*, 7238.

(76) Kim, Y.-K.; Koo, J. P.; Ha, J. S. *Appl. Surf. Sci.* **2005**, *249*, 7.